ingegneria sismica
International Journal of Earthquake Engineering
Anno XLIII - Num. 2 - 2026

Performance optimization and dynamic behavior analysis of a novel rigid flexible coupled multibody mechanical system based on dynamic response characteristics

Lingtao Liu[1,*]

[1] School of Intelligent Manufacturing, Chongqing Vocational College of Light Industry,
Chongqing, 401329, China

SUMMARY: *This article aims to propose a novel performance optimization and dynamic behavior analysis method for rigid flexible coupled multibody mechanical systems based on dynamic response characteristics. Firstly, a multi-body system dynamics optimization model with singular positions is established using the Gaussian principle, transforming the dynamics problem into an optimization problem of finding the extremum of a function. Secondly, the Artificial Fish Swarm Optimization Algorithm (AFSA) is improved by proposing a hybrid algorithm (IAFSA) that combines intelligent optimization and traditional optimization methods to fully utilize the advantages of both and solve dynamic optimization models. This algorithm enhances the global search capability and convergence speed of the algorithm by adding feasible solutions from traditional unconstrained optimization and the optimal solution from the previous time step as additional fish swarm individuals, and introducing mutation operators. Finally, taking the planar flexible double pendulum system as an example, the effectiveness of the proposed method was verified through simulation experiments. The experimental results show that the IAFSA algorithm has higher accuracy and better optimization ability compared to the traditional AFSA algorithm when reverse calculating the initial state angle of the system, and the fitness function value is significantly reduced. Research has shown that the multi-body system dynamics optimization method based on Gaussian principle and improved artificial fish swarm algorithm proposed in this paper can effectively handle multi-body system dynamics problems with singular positions, and improve the accuracy and efficiency of system performance optimization.*

KEYWORDS: *rigid flexible coupled multi-body mechanical system; Dynamic response characteristics; Dynamic optimization model; Artificial fish swarm optimization algorithm; Flat flexible double pendulum system; System performance optimization*

1 Introduction

With the rapid development of modern mechanical industry, there is an increasing demand for reliability, response speed, accuracy, and lifespan of multi-body systems in precision mechanical engineering, aerospace, military and other fields, such as space folding mechanisms, multi axis parallel machine tools, industrial robots, aerospace structures, and high-end mechanical equipment [1, 2]. The improvement in various performance indicators required by these multi-body systems presents higher challenges and demands for the design and research of multi-body systems. To meet these challenges and requirements, researchers need to consider

---

*epkl2452@hotmail.com

https://doi.org/10.65102/is2026836

more factors that may affect the performance of the mechanism when designing multi-body systems, such as machining accuracy, form and position tolerances, working environment, and other factors that may affect the performance of the mechanism [3].

In multi-body system dynamics modeling, uncertain parameters are usually divided into random variables and interval variables. The distribution characteristics contained in random variables are precisely defined through probability distribution functions [4]. By using Monte Carlo simulation methods or polynomial chaos expansion techniques, the statistical characteristics of system response can be effectively derived. However, in practical application scenarios, obtaining sample distribution information corresponding to random parameters often faces great difficulties. Compared to other methods, interval analysis uses interval variables to describe the uncertainty of parameters, and only requires obtaining the upper and lower boundaries of the interval variables, making it more widely applicable. For multi-body mechanical systems with interval parameters, the scanning method stands out due to its simplicity and reliability. Using this method can accurately obtain the boundary range of the system response. However, this method has a significant drawback, that is, its computational cost will sharply increase exponentially with the increase of interval parameters. Reference [5] used the Taylor model method to study the response analysis of multi-body systems with interval parameters. Due to the difficulty of handling large uncertainty problems using Taylor expansion based methods, the subinterval technique divides the original interval into multiple subintervals to improve computational accuracy. To avoid the differentiation operation in Taylor expansion method. Reference [6] innovatively proposed the Chebyshev interval analysis method (CIM) based on Chebyshev polynomials, and successfully applied this method to the analysis of uncertain responses in multi-body systems. CIM approximates the relationship between the output response and input interval parameters at each moment using Chebyshev polynomials, and can be considered as a method based on surrogate models (SBM). The SBM method is dedicated to building proxy models with low computational costs, and then obtaining output response boundaries from the proxy models through scanning or optimization methods. Based on this concept, Reference [7] applies Legendre polynomials to the interval dynamic response analysis of automotive suspension systems. Reference [8] used arbitrary chaotic polynomials to study the interval response of the cannon power system. In addition, radial basis functions and kriging models are also applied to interval uncertainty analysis. Reference [9] uses the maximum entropy method to obtain statistical information on the output parameters of multi-body systems, and further uses Taylor expansion to obtain the response interval of the distribution function.

However, when faced with the task of dealing with long-term interval dynamic response problems, the uncertainty analysis methods based on alternative models usually gradually deteriorate over time. And this phenomenon occurs in both probabilistic and interval methods. In multi-body systems, when uncertain parameters take different values, the resulting system response also has different frequencies and phases [10]. In the process of analyzing uncertain dynamic responses associated with time, as time passes, the phase differences between the responses of each sample will gradually widen. The continuous increase of this phase difference will trigger the cumulative effect of instantaneous phase difference, thereby making the correlation between system response and uncertain parameters increasingly complex. Even if the proxy model has a high order, it is difficult to accurately approximate the intrinsic relationship between the response function and uncertain parameters in subsequent stages. This situation can lead to deviations between the obtained upper and lower limits and the actual boundary over time, ultimately resulting in a continuous boundary situation. For this reason, Reference [11] pioneered the integration of adaptive signal decomposition techniques into the uncertainty analysis system based on response surface methodology, and innovatively proposed two methods, RS-HT and RS-LMD. Compared to traditional response surface methods, this method can use low order polynomials to handle long-term uncertain dynamic response problems.

This article uses the Gaussian principle to establish a dynamic optimization model for multibody systems with singular positions, and directly solves it using mathematical optimization methods, transforming the dynamic problem of multibody systems with singular positions into an optimization problem of finding function extremum [12]. At present, the methods for solving optimization problems are mainly divided into two categories: the first category is traditional algorithms, which have high efficiency in solving convex problems but are not suitable for multi extremum problems, and the solutions are mostly local optima; Another type is intelligent algorithms, which have a certain degree of randomness and are suitable for multi-modal optimization problems. They have strong robustness and are not easily trapped in local optima. Fish swarm optimization algorithm (AFSA), as a stochastic optimization algorithm based on population mechanism, has attracted much attention in recent years' research and application, mainly due to its simple implementation process and significant ability to quickly converge to the optimal solution. It has been applied in fields such as artificial neural network training, functional optimization, fuzzy control, and pattern recognition. This article improves AFSA and combines intelligent optimization with traditional optimization methods, fully utilizing the fast convergence of traditional optimization and the global search characteristics of intelligent optimization. It solves the dynamic optimization model established by Gaussian method and explores its feasibility in solving dynamic singular position problems.

2 Related research

As an independent branch of classical mechanics, the study of multibody system dynamics has demonstrated significant importance in the fields of complex mechanics, aerospace, and robotics applications. Multibody system refers to a complex mechanical system composed of several objects with rigid or flexible characteristics that are interconnected through motion pairs. The field of multibody system dynamics mainly focuses on in-depth exploration of the dynamic characteristics and motion laws exhibited by multiple entities [13].

The study of multibody system dynamics originated in the early 1960s. Reference [14] introduces topological structures into multibody systems and applies graph theory related knowledge to describe the kinematics and dynamics of multibody systems, enabling computers to distinguish the relationships between entities in multibody systems. Based on the Euler Lagrange equation and variational method, numerical calculations can be directly used to study the motion laws of multibody systems when solving dynamic equations. Reference [15] studied the rigid motion of two satellites under the action of gravitational torque, and derived the corresponding motion equations using the Newton Euler equation, thus establishing the corresponding dynamic equations for the system. Reference [16] applied the Newton Euler equation to the dynamic study of satellite mechanical systems, greatly promoting the application of the Newton Euler equation in multibody systems and laying a good foundation for the development of multibody system dynamics in the early stages. Reference [17] proposed a method for explicitly eliminating constraint torques in a typical n vector equation system of satellite attitude dynamics composed of n arbitrarily connected rigid bodies using Newton Euler equations. Poinsot proposed the spinor theory in the early 19th century and received Ball's systematic development in 1876. Using spinor theory, he conducted in-depth research on the kinematics and dynamics of rigid bodies under composite constraints. Reference [18] proposed the natural coordinate method, also known as the fully Cartesian coordinate method. This method uses Cartesian coordinates of a point system to characterize the spatial layout of a multibody system, while using natural coordinates to represent the attitude states of each rigid body within the multibody system, thereby constructing the dynamic equations of the multibody system. Reference [19] innovatively proposed a theory for constructing dynamic equations of multi degree of freedom systems, which is named the Kane method. This method is unique in that it sets the generalized velocity as the independent variable to accurately describe the motion state of multi-body systems. Moreover, utilizing the D'Alembert principle to construct a framework for the dynamic equations of multibody systems significantly reduces the complexity of the calculation process. Reference [20] proposed an effective concept for solving the motion equations of flexible multi-body systems, further supplementing and improving the Kane method. Reference [21] established dual dynamic equations based on dual vectors and spiral calculus, providing a concise analytical tool for studying rigid body dynamics in multibody systems. Relatively speaking, the absolute coordinate method assumes that all rigid bodies in a multibody system are in a free state, and then uses the center position and attitude of each rigid body as the absolute coordinates of the multibody system to establish dynamic equations for each rigid body, and finally calculates them through Lagrange multipliers.

With the continuous improvement of multi-body system dynamics theory, flexible multi-body system dynamics theory including flexible bodies has gradually been widely studied. The dynamic modeling method of multi rigid body systems is based on the premise that each rigid body will not deform. However, in flexible multibody systems, one or several flexible bodies will undergo varying degrees of deformation due to different materials or forces during motion. Given this, how to accurately characterize the deformation status of flexible bodies has become a key issue that many scholars are focusing on exploring [22]. According to the degree of deformation of flexible bodies, they can be divided into two categories: small deformation and large deformation. In the method system for describing flexible deformation, commonly used methods include floating coordinate system method, absolute node coordinate method, and recursive method. The so-called floating coordinate system refers to a coordinate system that cannot be fixed at a certain point within the deformable body and remains "floating" within the deformable body. The floating coordinate system method is mainly used to deal with small deformation problems. In flexible multibody systems, the motion of objects can be decomposed into floating coordinate system motion in a wide range of scenes, as well as their own elastic deformation motion. Based on this characteristic, the floating coordinate system has the feasibility of serving as a reference coordinate system for analyzing the motion of deformable bodies. The absolute node coordinate method is based on the finite element method, using the absolute coordinates in the reference coordinates to define the coordinates of the element nodes, and representing the node's rotation angle through the slope vector. This method has shown good applicability in handling large deformation problems, especially for large deformation situations in flexible multibody systems. The recursive method cleverly combines the strengths of the floating coordinate system method and the absolute node coordinate system method. It uses a recursive operation process to convert absolute coordinates into relative coordinates, and successfully constructs the dynamic equations of multi-body systems.

3 General form of multi-body system dynamics equations

3.1 Kinematic Equations of Multibody Systems

The primary task in constructing the kinematic equations of a multibody system is to deduce the kinematic relationship between two adjacent rigid bodies. The specific motion relationship between two adjacent rigid bodies can refer to the content presented in Figure 1. In Figure 1,

$O_0x_0y_0z_0$ is the reference coordinate system, $O_ix_iy_iz_i$ and $O_jx_jy_jz_j$ are the connected coordinate systems on B_i and B_j rigid bodies respectively, and $p_{iO}\xi_{iO}\eta_{iO}\zeta_{iO}$ and $p_{jI}\xi_{jI}\eta_{jI}\zeta_{jI}$ are the coordinate systems where hinge J_j is connected to rigid bodies B_i and B_j respectively.

Assuming that the velocity and acceleration vectors of the connected coordinate systems $O_ix_iy_iz_i$ and $O_jx_jy_jz_j$ of bodies B_i and B_j relative to the reference coordinate system $O_0x_0y_0z_0$ are:

$$\begin{cases} \boldsymbol{S}_i = \begin{bmatrix} \boldsymbol{\omega}_i \\ \boldsymbol{v}_i \end{bmatrix}, \boldsymbol{S}_j = \begin{bmatrix} \boldsymbol{\omega}_j \\ \boldsymbol{v}_j \end{bmatrix} \\ \dot{\boldsymbol{S}}_i = \begin{bmatrix} \boldsymbol{\varepsilon}_i \\ \boldsymbol{a}_i \end{bmatrix}, \dot{\boldsymbol{S}}_j = \begin{bmatrix} \boldsymbol{\varepsilon}_j \\ \boldsymbol{a}_j \end{bmatrix} \end{cases} \tag{1}$$

where, $\boldsymbol{\omega}$, $\boldsymbol{\varepsilon}$, $\boldsymbol{v}$, and $\boldsymbol{a}$ represent the angular velocity, angular acceleration, linear velocity, and linear acceleration of the connected coordinate system, respectively; The subscripts *i* and *j* represent the number of the body. The relative velocity and relative acceleration vectors between the hinge coordinate system $p_{jI}\xi_{jI}\eta_{jI}\zeta_{jI}$ and $p_{iO}\xi_{iO}\eta_{iO}\zeta_{iO}$ are $\dot{\boldsymbol{q}}_j$ and $\ddot{\boldsymbol{q}}_j$, respectively.

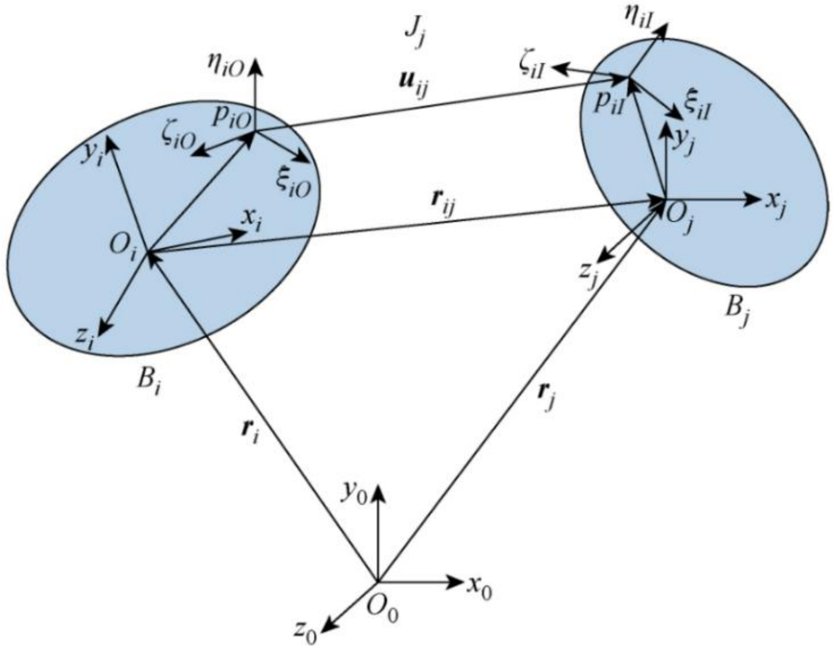

Figure 1: Position relationship between adjacent rigid bodies

According to the relative coordinate method, the relationship between the motion vector of the body coordinate system and the relative motion vector can be recursively derived:

$$\begin{cases} \boldsymbol{S}_j = \boldsymbol{T}_j\boldsymbol{S}_i + \boldsymbol{D}_j\dot{\boldsymbol{q}}_j \\ \dot{\boldsymbol{S}}_j = \boldsymbol{T}_j\dot{\boldsymbol{S}}_i + \dot{\boldsymbol{T}}_j\boldsymbol{S}_i + \boldsymbol{D}_j\ddot{\boldsymbol{q}}_j + \dot{\boldsymbol{D}}_j\dot{\boldsymbol{q}}_j \end{cases} \tag{2}$$

where, $\boldsymbol{T}_j$, $\dot{\boldsymbol{T}}_j$, $\boldsymbol{D}_j$, and $\dot{\boldsymbol{D}}_j$ are the corresponding recursive relationship matrices obtained using the relative coordinate method. According to equation (2), assuming there are N individuals in total, the motion relationship of all bodies in a multi-body system can be obtained by synthesizing the equations:

$$\begin{cases} \boldsymbol{S} = \boldsymbol{H}\dot{\boldsymbol{q}} \\ \dot{\boldsymbol{S}} = \boldsymbol{H}\ddot{\boldsymbol{q}} + \dot{\boldsymbol{H}}\dot{\boldsymbol{q}} \end{cases} \tag{3}$$

where, $\dot{\boldsymbol{q}} = [\dot{\boldsymbol{q}}_1, \dot{\boldsymbol{q}}_2, \cdots, \dot{\boldsymbol{q}}_N]^{\mathrm{T}}$; $\ddot{\boldsymbol{q}} = [\ddot{\boldsymbol{q}}_1, \ddot{\boldsymbol{q}}_2, \cdots, \ddot{\boldsymbol{q}}_N]^{\mathrm{T}}$; $\boldsymbol{S} = [\boldsymbol{S}_1, \boldsymbol{S}_2, \cdots, \boldsymbol{S}_N]^{\mathrm{T}}$; $\dot{\boldsymbol{S}} = [\dot{\boldsymbol{S}}_1, \dot{\boldsymbol{S}}_2, \cdots, \dot{\boldsymbol{S}}_N]^{\mathrm{T}}$; H is the corresponding coefficient matrix.

3.2 Multibody System Dynamics Equations

For any rigid body B_i, assuming $\boldsymbol{c}_i$ is the radial vector of any point in the body relative to the connected coordinate system $O_i x_i y_i z_i$, the acceleration of that point can be obtained as:

$$\boldsymbol{a}_{c_i} = \boldsymbol{a}_i + \boldsymbol{\varepsilon}_i \times \boldsymbol{c}_i + \boldsymbol{\omega}_i \times (\boldsymbol{\omega}_i \times \boldsymbol{c}_i) \tag{4}$$

where, $\boldsymbol{a}_i$ is the acceleration of O_i relative to the reference coordinate system $O_0 x_0 y_0 z_0$.

Based on the principle of virtual power, the virtual power equation corresponding to an object can be derived in the following specific form:

$$\int_V \delta \boldsymbol{v}_{c_i}^{\mathrm{T}} \left(\rho \boldsymbol{a}_{c_i} + \boldsymbol{F}_i^{\mathrm{a}} + \boldsymbol{F}_i^{\mathrm{n}} \right) \mathrm{d}V = \boldsymbol{0} \tag{5}$$

where, $\boldsymbol{F}_i^{\mathrm{a}}$ and $\boldsymbol{F}_i^{\mathrm{n}}$ are the generalized external load and ideal hinge constraint load that the body is subjected to, respectively; ρ is the density of the body; $\delta \boldsymbol{v}_{c_i}$ is the virtual velocity, expressed as:

$$\delta \boldsymbol{v}_{c_i} = \delta \boldsymbol{v}_i + \delta (\boldsymbol{\omega}_i \times \boldsymbol{c}_i) \tag{6}$$

When the virtual power equation corresponding to a single unit is extended and applied to a multi-body system, and it is reasonably integrated and presented in a compact form, the following results can be derived:

$$\delta \boldsymbol{S}^{\mathrm{T}} \boldsymbol{R} \dot{\boldsymbol{S}} + \delta \boldsymbol{S}^{\mathrm{T}} \boldsymbol{WRES} = \delta \boldsymbol{S}^{\mathrm{T}} \boldsymbol{Q}^{\mathrm{a}} + \delta \boldsymbol{S}^{\mathrm{T}} \boldsymbol{Q}^{\mathrm{n}} \tag{7}$$

where, $\boldsymbol{R}$, $\boldsymbol{W}$, $\boldsymbol{E}$, $\boldsymbol{Q}^{\mathrm{a}}$, and $\boldsymbol{Q}^{\mathrm{n}}$ are the integrated forms of each term in equation (5) in the entire multi-body system.

Substituting equation (3) into equation (7) yields:

$$\delta \dot{\boldsymbol{q}}^{\mathrm{T}} \boldsymbol{H}^{\mathrm{T}} \boldsymbol{R} \boldsymbol{H} \ddot{\boldsymbol{q}} + \delta \dot{\boldsymbol{q}}^{\mathrm{T}} \boldsymbol{H}^{\mathrm{T}} (\boldsymbol{R} \dot{\boldsymbol{H}} + \boldsymbol{WREH}) \dot{\boldsymbol{q}} = \delta \dot{\boldsymbol{q}}^{\mathrm{T}} \boldsymbol{H}^{\mathrm{T}} \boldsymbol{Q}^{\mathrm{a}} + \delta \dot{\boldsymbol{q}}^{\mathrm{T}} \boldsymbol{H}^{\mathrm{T}} \boldsymbol{Q}^{\mathrm{n}} \tag{8}$$

Given that the constraint force and torque do not produce any work effect in the relevant process, the corresponding virtual power value is 0. Write equation (8) in a compact form to obtain:

$$\delta \dot{\boldsymbol{q}}^{\mathrm{T}} \boldsymbol{M} \ddot{\boldsymbol{q}} + \delta \dot{\boldsymbol{q}}^{\mathrm{T}} \boldsymbol{C} \dot{\boldsymbol{q}} = \delta \dot{\boldsymbol{q}}^{\mathrm{T}} \boldsymbol{F} \tag{9}$$

Based on the principle of variation, the dynamic equations of the system can be derived in the following way:

$$\boldsymbol{M}\ddot{\boldsymbol{q}}+\boldsymbol{C}\dot{\boldsymbol{q}}=\boldsymbol{F} \tag{10}$$

When a multi-body system contains complete constraints, the dynamic equation with constraints is written by introducing Lagrange multipliers:

$$\begin{cases}\boldsymbol{M}(\boldsymbol{q},t)\ddot{\boldsymbol{q}}+\boldsymbol{C}(\boldsymbol{q},\dot{\boldsymbol{q}},t)\dot{\boldsymbol{q}}+\boldsymbol{\Phi}_q^{\mathrm{T}}\boldsymbol{\lambda}=\boldsymbol{F}\\ \boldsymbol{\Phi}(\boldsymbol{q},t)=\mathbf{0}\end{cases} \tag{11}$$

where, $\boldsymbol{\Phi}(\boldsymbol{q},t)=\mathbf{0}$ is the system constraint equation; $\boldsymbol{\Phi}_q$ is the derivative of $\boldsymbol{\Phi}(\boldsymbol{q},t)$ and $\boldsymbol{q}$. Calculate the second derivative of the constraint equation $\boldsymbol{\Phi}(\boldsymbol{q},t)=\mathbf{0}$ with respect to time t in equation (11).

3.3 Dynamic optimization model based on Gaussian principle

The Gauss principle is a fundamental variational principle [23]. Compared with other integral variational principles, as a differential variational principle with acceleration as the variable, the Gaussian principle can more conveniently transform the dynamic problems of multibody systems into the problem of finding the minimum value of a constrained function, and thus use mathematical optimization algorithms to handle it.

The Gaussian principle can be described in the form of the minimum value: at any given moment, the true motion of a system is compared with possible motions with the same position and velocity. Therefore, the Gaussian principle is also known as the Gaussian minimum constraint principle. Where, The constraint function is a measure of the deviation of the true motion of a system from free motion.

Assuming the system consists of *N* particles, where m_i and $\ddot{\boldsymbol{r}}_i$ are the mass and acceleration of the *i*-th center of mass, the constraint function is expressed as follows:

$$G=\frac{1}{2}\sum_{i=1}^{N}m_i\left(\ddot{\boldsymbol{r}}_i-\frac{\boldsymbol{F}_i}{m_i}\right)^2 \tag{12}$$

For the above particle system, *n* coordinates $q_1,q_2,\cdots,q_n$ are selected as the generalized coordinates of the system, and the selected generalized coordinates may not be independent of each other. The radius of a particle can be expressed in generalized coordinates as:

$$r_{\mathrm{i}}=r_{\mathrm{i}}\left(q_1,q_2,\cdots,q_n\right) \tag{13}$$

Unfolding the constraint represented by equation (12) yields:

$$G=\frac{1}{2}\sum_{i=1}^{N}\left(m_i\ddot{\boldsymbol{r}}_i\cdot\ddot{\boldsymbol{r}}_i-2\ddot{\boldsymbol{r}}_i\cdot\boldsymbol{F}_i+m_i^{-1}\boldsymbol{F}_i\cdot\boldsymbol{F}_i\right) \tag{14}$$

Furthermore, a constraint function in the form of generalized coordinates can be obtained:

$$G=\frac{1}{2}(\boldsymbol{M}\ddot{\boldsymbol{q}}-\boldsymbol{Q})^{\mathrm{T}}\boldsymbol{M}^{-1}(\boldsymbol{M}\ddot{\boldsymbol{q}}-\boldsymbol{Q}) \tag{15}$$

The generalized acceleration of the system can be obtained by solving the following constrained optimization problem:

$$\ddot{\boldsymbol{q}} = \arg\min\left\{\frac{1}{2}(\boldsymbol{M}\ddot{\boldsymbol{q}}-\boldsymbol{Q})^{\mathrm{T}}\boldsymbol{M}^{-1}(\boldsymbol{M}\ddot{\boldsymbol{q}}-\boldsymbol{Q})\boldsymbol{C}_q\ddot{\boldsymbol{q}} = -\boldsymbol{\eta}\right\} \tag{16}$$

4 Dynamic model optimization based on improved artificial fish swarm algorithm

4.1 Introduction to artificial fish swarm algorithm

In order to solve constrained optimization problems, scholars have developed different deterministic and stochastic algorithms. Given that deterministic methods (such as feasible direction method and generalized gradient descent method) impose strict assumptions on the continuity and differentiability of the objective function, which are difficult to fully satisfy in practical problems, their applicability is limited. With the development of optimization theory, some intelligent algorithms have rapidly developed and been widely applied, providing practical and feasible solutions for complex functions and combinatorial optimization problems with nonlinearity and multiple extremum [24].

The Artificial Fish Swarm Optimization Algorithm (AFSA), as a heuristic global optimization technique (see Figure 2), can simulate the hunting behavior of fish schools randomly searching for food. Fish schools will dynamically adjust their search routes based on their accumulated exploration experiences and information exchange among group members, in order to explore food resources. In each search process of the fish swarm optimization algorithm, the algorithm will flexibly change its search direction and speed based on the individual's own experience (i.e. the optimal position reached by the individual in the past search process) and the information obtained from group communication (i.e. the best position recorded by the individual in historical searches), in order to achieve the goal of exploring the optimal solution.

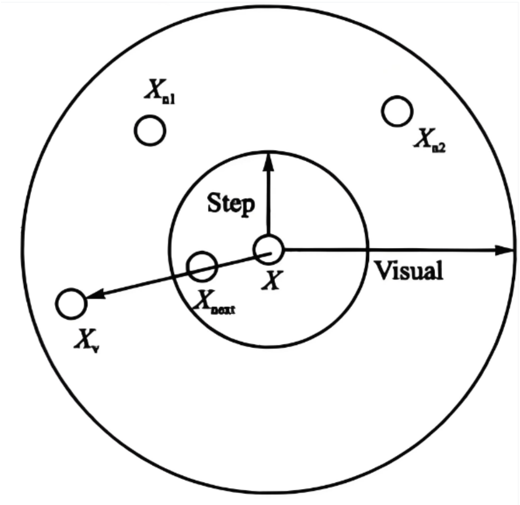

Figure 2: Artificial Fish Swarm Optimization Algorithm

The AFSA algorithm has the following three basic behaviors:

(1) Foraging behavior: Individual fish X_i randomly selects the next state X_j within a perceptible area. If the food concentration value in the next state is better, move to the X_j state position. Otherwise, select a new state. If the better state cannot be found after multiple attempts, randomly select a state.

(2) Crowding behavior: Add up the state vectors of all artificial fish in the field of view and take the average to obtain the center position. Compare the food concentration values of individual artificial fish with those of the clustered position. If the food concentration value of the clustered position is better, move towards the center position.

(3) Rear end behavior: Individual fish X_i searches for individual fish X_j with the best food concentration value within a perceptible area. If the food concentration value of individual fish X_j is better than that of individual fish X_i, it moves towards individual fish X_j.

4.2 Model solving process

This article improves the classic AFSA by adding a feasible solution from traditional unconstrained optimization and the optimal solution from the previous time step as additional fish populations to the initial fish population, based on reference [25], in order to achieve fast convergence and global optimization. In response to the expansion of the solution space caused by singular positions, this paper introduces mutation operators into the artificial fish swarm optimization algorithm to further increase the diversity of the fish swarm population, enabling the algorithm to quickly jump out of local optima and prevent premature convergence. The new artificial fish swarm algorithm is as follows [26, 27]:

$$\boldsymbol{v}_{id}^{k+1} = \boldsymbol{w}\times\boldsymbol{v}_{id}^{k} + c_1\times\text{rand}()\times\left(\boldsymbol{p}_{id}^{k}-\boldsymbol{x}_{id}^{k}\right)+c_2\times\text{rand}()\times\left(\boldsymbol{p}_{gd}^{k}-\boldsymbol{x}_{id}^{k}\right)c_2+\rho\,\text{rand}()\times\left(\text{rand}()-\boldsymbol{x}_{id}^{k}\right) \tag{17}$$

where, ρ is the variation factor, with a value of 2.

The operation process for simulating multi-body systems with singular positions is as follows [28].

1) Given the simulation time t_{end} and time step $\vartriangle t$ in advance, provide the initial conditions that satisfy the constraint equation, velocity $\dot{\boldsymbol{q}}_0$ and displacement $\boldsymbol{q}_0$, and let $t = t_0$.

2) Calculate the quality matrix $\boldsymbol{M}$ of the system, including the generalized torque matrix $\boldsymbol{Q}$ of external force and velocity related terms, the Jacobian matrix $\boldsymbol{C}_q$ of the constraint equation, and the right-hand term $\boldsymbol{\eta}$ of the constraint equation.

3) Establish a dynamic model of a multibody system using equation (16), and solve for the acceleration of the system according to the following steps.

3-1) Let *k*=0, initialize the *d*-dimensional fish swarm individuals X^k that satisfy the constraint conditions, and let the initial velocity $\boldsymbol{V}^k = \boldsymbol{0}$ of all fish swarm individuals.

3-2) Obtain the optimal solution $\boldsymbol{x}_0$ of the unconstrained objective function and update the last individual fish swarm to $\boldsymbol{X}_\tau = \boldsymbol{x}_0$; If k=0, then $\boldsymbol{X}_{\tau-1} = \boldsymbol{x}_0$, otherwise $\boldsymbol{X}_{\tau-1} = \boldsymbol{q}_{t-1}$.

3-3) Assign the optimal position of the current fish group individual to GG:

$\boldsymbol{P}^k = \boldsymbol{X}^k$

3-4) Evaluate the objective function value $\boldsymbol{f}_k\left(\boldsymbol{P}^k\right)$ of each individual fish group, find the optimal value, and assign it to $\boldsymbol{P}_\text{g}^k$:

$$\boldsymbol{P}_\text{g}^k = \arg\min\left\{\boldsymbol{f}_k\left(\boldsymbol{P}^k\right)\right\}$$

3-5) Let *k*=*k*+1 and update the individual velocity $\boldsymbol{V}^k$ and position $\boldsymbol{P}^k$ of the fish swarm.

3-6) Update the historical optimal position $\boldsymbol{P}^k$ and the optimal individual position $\boldsymbol{P}_\text{g}^k$ of each fish group:

$$\boldsymbol{P}_i^k = \begin{cases} \boldsymbol{P}_i^{k-1}, & f\left(\boldsymbol{X}_i^k\right) \geq f\left(\boldsymbol{P}_i^{k-1}\right) \\ \boldsymbol{X}_i^k, & f\left(\boldsymbol{X}_i^k\right) < f\left(\boldsymbol{P}_i^{k-1}\right) \end{cases}$$

$$\boldsymbol{P}_g^k = \begin{cases} \boldsymbol{P}_g^{k-1}, & f\left(\boldsymbol{X}_i^k\right) \geq f\left(\boldsymbol{P}_g^{k-1}\right) \\ \boldsymbol{X}_i^k, & f\left(\boldsymbol{X}_i^k\right) < f\left(\boldsymbol{P}_g^{k-1}\right) \end{cases}$$

3-7) Go to step 3-3 until *k* meets the condition or $\left\|\boldsymbol{P}_{\mathrm{g}}^k - \boldsymbol{P}_{\mathrm{g}}^{k-1}\right\| < \varepsilon$, and return the optimal individual value $\boldsymbol{P}_g^k$ of the fish swarm to the group.

4) Integrate the acceleration $\ddot{\boldsymbol{q}}_t$ to obtain the velocity $\dot{\boldsymbol{q}}_{t+\Delta t}$ and displacement $\boldsymbol{q}_{t+\Delta t}$ at the next moment, and make $t = t + \Delta t$.

5) If $t > t_{\mathrm{end}}$, the program terminates; otherwise, go to step 2.

5 Experimental analysis

The initial state of the planar flexible double pendulum system is shown in Figure 3, and its characteristic parameters are shown in Table 1. The lengths of pole OA and pole AB are 1 and 2 m, respectively, with a cross-sectional area of (0.04 × 0.02) m^2 and a density of 5540 kg/m^2. The Young's moduli of rods OA and AB are 2 × 10^8 and 2 × 10^7 Pa, respectively, with a Poisson's ratio of 0.3 for both. Two and four absolute node coordinate formulas are respectively used to discretize the flexible rods OA and AB in the fully parameterized beam element, and the rods OA and AB only move under the action of gravity. During the calculation process, the integration time step is 5 × 10-4s.

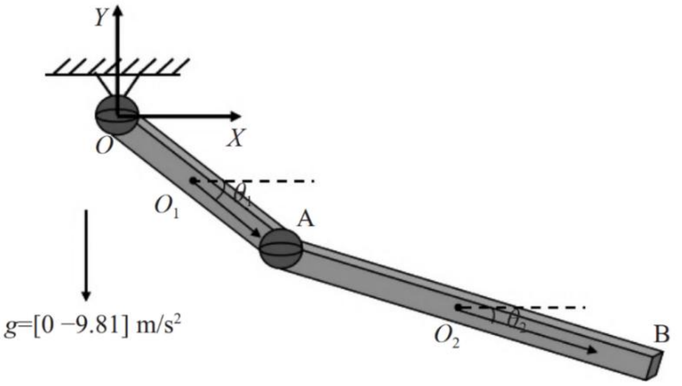

Figure 3: Planar Flexible Double Pendulum System

Table 1: Characteristic parameters of planar flexible double pendulum system

Component Name	Length/m	Cross sectional area/m^2	Density/(kg×m^{-3})	Young's modulus/Pa	Poisson's ratio	Unit number
Pole OA	1	0.04×0.02	5540	2×10^8	0.3	2
Rod AB	2	0.04×0.02	5540	2x10^7	0.3	4

The dynamic forward problem of a flexible multibody system can be described as calculating the displacement of the end point B of the double pendulum system in the X and Y directions based on the angles θ_1 and θ_2 between the rods OA and AB and the X direction (horizontal direction), as well as the system parameters given in Table 1, under known initial states. Figure 4 shows the sensitivity analysis results of the X and Y direction displacements of point B with respect to the initial state angle and after 0.5 seconds of motion in the double pendulum system.

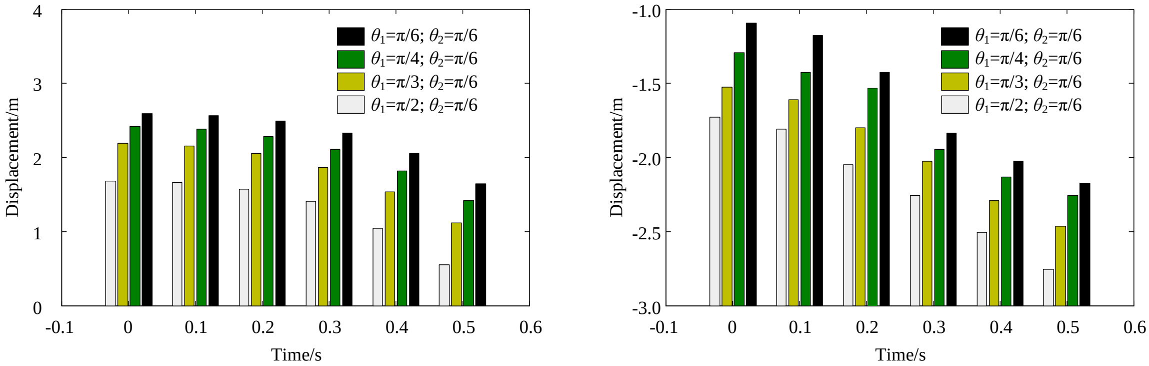

(a) The variation of displacement in the X direction of point B with angle θ1

(b) The variation of Y-direction displacement of point B with angle θ1

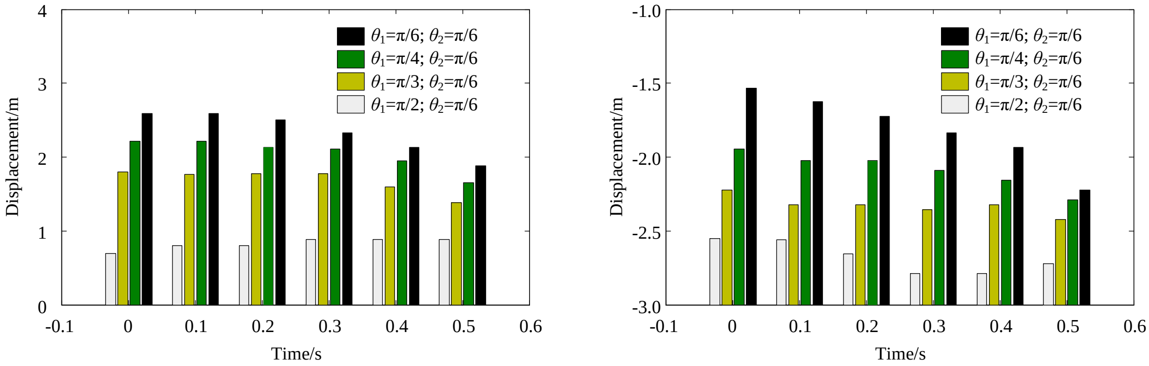

(c) The variation of displacement in the X direction of point B with angle θ2

(d) The variation of Y-direction displacement of point B with angle θ2

Figure 4: Sensitivity analysis results

Figures 4 (a) and (b) respectively show the displacement of point B in the X and Y directions as the angle θ_2 remains constant; Figures 4 (c) and (d) respectively show the displacement of point B in the X and Y directions with respect to angle θ_2, while keeping angle θ_1 constant. From Figure 4, it can be seen that the displacement of point B in the X and Y directions at the end of the double pendulum system is sensitive to the initial state angle and, in other words, there is a strong causal relationship between them. In addition, even in the same initial state, the trajectory of the double pendulum movement is almost different each time. Therefore, for solving the inverse problem of the dynamics of a double pendulum system, it is necessary to specify the motion trajectory of the double pendulum system.

Below are the performance optimization and dynamic behavior analysis results of multi-body mechanical systems under two operating conditions:

(1) The result in the first operating condition (Case 1) is calculated from the forward problem with initial states of $\theta_1 = \pi/4(\approx 0.7854)\text{rad}$ and $\theta_2 = \pi/6(\approx 0.5236)\text{rad}$ [29, 30]. Assuming that the angle parameter of the initial state cannot be accurately measured, it is necessary to reverse calculate the initial state angle and θ_2 based on the displacement in the X and Y directions of point B at multiple given time points. The results obtained by reverse

engineering using AFSA algorithm and IAFSA algorithm are shown in Table 2. In the example, the particle population size is set to 40 and the maximum number of iterations is 100. The results obtained from the reverse calculation of the two methods are almost identical, and the initial state angles obtained from the reverse calculation are $\theta_1 \approx 0.7854\text{rad}$ and $\theta_2 \approx 0.5236\text{rad}$, which are almost identical to the actual initial state angle parameters. In addition, the fitness function values of AFSA algorithm and IAFSA algorithm are 6.0323 × 10^{-6} and 1.6541 × 10^{-8}, respectively. The fitness function value of IAFSA algorithm is smaller, indicating that IAFSA algorithm has better optimization ability than AFSA algorithm.

Table 2: Reverse calculation results of initial state angle of deterministic planar double pendulum system (Case 1)

Optimization algorithm	The true value/rad of the initial state angle θ_1	Inverse evaluation/rad of initial state angle θ_1	The true value/rad of the initial state angle θ_2	The true value/rad of the initial state angle θ_2	Fitness function value
AFSA	$\frac{\pi}{4}(\approx 0.7854)$	0.7584	$\frac{\pi}{6}(\approx 0.5236)$	0.5236	6.0323×10-6
IAFSA	$\frac{\pi}{4}(\approx 0.7854)$	0.7584	$\frac{\pi}{6}(\approx 0.5236)$	0.5236	1.6541×10-8

(2) The result of the second operating condition (Case 2) was calculated from the forward problem with initial states of $\theta_1 = \pi/3(\approx 1.0472)\text{rad}$ and $\theta_2 = \pi/4(\approx 0.7854)\text{rad}$. The results obtained by reverse engineering using AFSA algorithm and IAFSA algorithm are shown in Table 3. In the example, the particle population size is set to 40, and the maximum number of iterations is 100. The inverse results of the two methods are almost identical. The initial state angles obtained by reverse engineering are $\theta_1 \approx 1.0472\text{rad}$ and $\theta_2 \approx 0.7854\text{rad}$, respectively. The fitness function values of AFSA algorithm and IAFSA algorithm are 6.6317 × 10^{-7} and 2.1591 × 10^{-8}, respectively. Compared with the AFSA algorithm, the fitness function value of the IAFSA algorithm is smaller, which fully demonstrates that the IAFSA algorithm has better optimization ability.

Table 3: Reverse calculation results of initial state angle of deterministic planar double pendulum system (Case 2)

Optimization algorithm	The true value/rad of the initial state angle θ_1	Inverse evaluation/rad of initial state angle θ_1	The true value/rad of the initial state angle θ_2	The true value/rad of the initial state angle θ_2	Fitness function value
AFSA	$\frac{\pi}{3}(\approx 1.0472)$	1.0472	$\frac{\pi}{4}(\approx 0.7854)$	0.7584	6.6317×10-7
IAFSA	$\frac{\pi}{3}(\approx 1.0472)$	1.0472	$\frac{\pi}{4}(\approx 0.7854)$	0.7584	2.1591×10-8

6 Conclusion

This article focuses on the performance optimization and dynamic behavior analysis of a novel rigid flexible coupled multibody mechanical system based on dynamic response characteristics, aiming to provide more effective theoretical and methodological support for the design and research of multibody systems. Firstly, a multi-body system dynamics optimization model with singular positions was successfully constructed using Gaussian principle, ingeniously transforming complex multi-body system dynamics problems into optimization problems for finding function extremum. Secondly, innovative improvements were made to the Artificial Fish Swarm Optimization Algorithm (AFSA), proposing a hybrid algorithm combining intelligent optimization and traditional optimization methods (IAFSA). This algorithm significantly enhances the global search capability and convergence speed of the algorithm by adding feasible solutions from traditional unconstrained optimization and the optimal solution from the previous time step as additional fish swarm individuals, and introducing mutation operators. Finally, taking the planar flexible double pendulum system as an example, simulation experiments were conducted. The experimental results showed that the multi-body system dynamics optimization method based on Gaussian principle and improved artificial fish swarm algorithm proposed in this paper can effectively handle multi-body system dynamics problems with singular positions, significantly improving the accuracy and efficiency of system performance optimization.

However, some areas for improvement were also identified during the research process. In terms of model construction, current research mainly focuses on specific types of multibody systems. For more complex and general multibody systems, the applicability and accuracy of dynamic optimization models need further verification and optimization. In terms of algorithm improvement, although the IAFSA algorithm has improved its global search ability and convergence speed, it still faces the problem of low computational efficiency when dealing with large-scale and high-dimensional optimization problems. Further research can be conducted on how to optimize the algorithm structure and improve computational performance. In addition, this article mainly takes the planar flexible double pendulum system as an example for experimental verification. In the future, more different types of multi-body system experiments can be expanded to more comprehensively evaluate the effectiveness of the proposed method.

Author's Profile

Lingtao Liu, Master, currently a Lecturer and Program Leader of Mechatronics Technology at Chongqing Vocational College of Light Industry. His research expertise includes multibody system dynamics, design and optimization of mechanical and electrical equipment. He maintains close cooperation with Chongqing Municipal Education Commission and China Non-Government Education Association, and works on research projects such as multi-objective optimization of composite machine tools for grinding and polishing of complex surfaces based on response surface methodology, analysis of casting defects in thin-walled aluminum alloy parts for new energy vehicles, and exploration of upgrading paths for mechatronics majors in vocational education oriented towards intelligent manufacturing. He has published several high-impact papers in the fields of mechanical equipment design and optimization, and multibody system dynamics.

References

[1] Hengstenberg S M, Robin C E P, Savage M J. Multi-body entanglement and information rearrangement in nuclear many-body systems: a study of the Lipkin–Meshkov–Glick model[J]. The European Physical Journal A, 2023, 59(10): 231.

[2] Smith T R, Bosanac N. Constructing motion primitive sets to summarize periodic orbit families and hyperbolic invariant manifolds in a multi-body system[J]. Celestial Mechanics and Dynamical Astronomy, 2022, 134(1): 7.

[3] Smith T R, Bosanac N. Motion Primitive Approach to Spacecraft Trajectory Design in a Multi-body System[J]. The Journal of the Astronautical Sciences, 2023, 70(5): 34.

[4] Arranz G, Martínez-Muriel C, Flores O, et al. Fluid–structure interaction of multi-body systems: Methodology and applications[J]. Journal of Fluids and Structures, 2022, 110: 103519.

[5] Lim M X, VanSaders B, Jaeger H M. Acoustic manipulation of multi-body structures and dynamics[J]. Reports on progress in physics, 2024, 87(6): 064601.

[6] Rahnejat H, Johns-Rahnejat P M, Dolatabadi N, et al. Multi-body dynamics in vehicle engineering[J]. Proceedings of the Institution of Mechanical Engineers, Part K: Journal of Multi-body Dynamics, 2024, 238(1): 3-25.

[7] Caruso M, Bregant L, Gallina P, et al. Design and multi-body dynamic analysis of the Archimede space exploration rover[J]. Acta Astronautica, 2022, 194: 229-241.

[8] Bruchko K L, Bosanac N. Rapid Trajectory Design in Multi-body Systems Using Sampling-Based Kinodynamic Planning: KL Bruchko, N. Bosanac[J]. The Journal of the Astronautical Sciences, 2025, 72(4): 33.

[9] Yap E J H, Rezgui D, Lowenberg M H, et al. Modeling flexible multi-body systems within the Udwadia–Kalaba framework, A lumped parameter approach[J]. Journal of Computational and Nonlinear Dynamics, 2022, 17(12): 121005.

[10] Rassaerts L, Suichies E, van de Vrande B, et al. Non-conservative obstacle avoidance for multi-body systems leveraging convex hulls and predicted closest points[C]//2025 IEEE International Conference on Robotics and Automation (ICRA). IEEE, 2025: 3007-3014.

[11] Hallak T S, Gaspar J F, Soares C G. A mathematical model for the dynamic analysis of multi-body floating platforms with complex mechanical constraints[J]. Ocean Engineering, 2024, 314: 119640.

[12] Amouzadrad P, Mohapatra S C, Soares C G. Review of recent developments on the hydroelastic response and gap resonance of multi-body floating structures[J]. Ocean Engineering, 2024, 313: 119398.

[13] Srinivasu N, Hashkavaei N S, Sanyal A K, et al. Coordinated Relative Attitude Control and Synchronization of a Multi-body Network of Vehicles[C]//2025 American Control Conference (ACC). IEEE, 2025: 1198-1203.

[14] van der Zanden J, Bunnik T, Cortés A, et al. Wave basin tests of a multi-body floating PV system sheltered by a floating breakwater[J]. Energies, 2024, 17(9): 2059.

[15] Lande-Sudall D R, Nyland J, Rykkje T R, et al. Hydrodynamic modelling of a multi-body wave energy converter using the Moving Frame Method[J]. Marine Structures, 2023, 87: 103332.

[16] Sidhoum Y, Oguri K. Low-thrust trajectory design for icy moons orbiters using multi-body techniques[J]. Celestial Mechanics and Dynamical Astronomy, 2024, 136(6): 55.

[17] Débarbouillé A, Renaud F, Dimitrijevic Z, et al. Wheel forces estimation with an Augmented and Constrained Extended Kalman Filter applied on a nonlinear multi-body model of a half vehicle[J]. Procedia Structural Integrity, 2022, 38: 342-351.

[18] Maciejewski I, Błażejewski A, Pecolt S, et al. Multi-body Model Simulating Biodynamic Responseof the Seated Human under Whole-Body Vibration[J]. Procedia Computer Science, 2022, 207: 227-234.

[19] Naito T, Naito H, Hashimoto K. Multi-body wave function of ground and low-lying excited states using unornamented deep neural networks[J]. Physical Review Research, 2023, 5(3): 033189.

[20] Karani M M H, Nikoo M R, Pirooz H D, et al. Multi-objective evolutionary framework for layout and operational optimization of a multi-body wave energy converter[J]. Energy, 2024, 313: 134045.

[21] Krot P, Shiri H, Dąbek P, et al. Diagnostics of bolted joints in vibrating screens based on a multi-body dynamical model[J]. Materials, 2023, 16(17): 5794.

[22] Balena M, Mantriota G, Reina G. Dynamic handling characterization and set-up optimization for a formula SAE race car via multi-body simulation[J]. Machines, 2021, 9(6): 126.

[23] Salgado A, Wdowicz D, Fernandes F, et al. Assessing head injury risks in electric scooter accidents: A multi-body simulation study with insights into sex differences[J]. Legal Medicine, 2024, 71: 102526.

[24] Bertetto A M, Melchiorre J, Marano G C. Improved multi-body rope approach for free-form gridshell structures using equal-length element strategy[J]. Automation in Construction, 2024, 161: 105340.

[25] Leith J, Russell R P. A time regularization scheme for spacecraft trajectories subject to multi-body gravity[J]. The Journal of the Astronautical Sciences, 2023, 70(2): 7.

[26] Caimi A, Ferguson S J, Ignasiak D. Evaluation of trunk muscle coactivation predictions in multi-body models[J]. Journal of Biomechanics, 2024, 168: 112039.

[27] Videbæk T E, Hayakawa D, Hagan M F, et al. Measuring multisubunit mechanics of geometrically programmed colloidal assemblies via cryo-EM multi-body refinement[J]. Proceedings of the National Academy of Sciences, 2025, 122(37): e2500716122.

[28] Adibzade M, Akbari H. Spectral approach to evaluate multi-body floating wave energy converters in complex sea states[J]. Ocean Engineering, 2023, 286: 115567.

[29] Koutras E, Moretti Leila F, Ribaric A, et al. A new contact and road model for multi-body dynamic simulation of wheeled vehicles on soft-soil terrain[J]. Multibody System Dynamics, 2025, 63(1): 39-62.

[30] Bock H G, Kostina E, Sauter M, et al. Numerical methods for diagnosis and therapy design of cerebral palsy by bilevel optimal control of constrained biomechanical multi-body systems[M]//Non-Smooth and Complementarity-Based Distributed Parameter Systems: Simulation and Hierarchical Optimization. Cham: Springer International Publishing, 2021: 21-41.